Preprints of the 21st IFAC World Congress (Virtual)
Berlin, Germany, July 12-17, 2020

Reserve Balancing in a Microgrid System for Safety Analysis ⋆

Clemens Kiebler * **Ionela Prodan** ** **Felix Petzke** * **Stefan Streif** *

* *Technische Universität Chemnitz, Automatic Control and System Dynamics Lab (e-mail: clemens.kiebler@s2014.tu-chemnitz.de, felix.petzke,stefan.streif@etit.tu-chemnitz.de).*
** *Univ. Grenoble Alpes, Grenoble INP ⋆, LCIS, F-26000 Valence (e-mail: ionela.prodan@lcis.grenoble-inp.fr)*

Abstract: This work presents a robust MPC (Model Predictive Control) approach for reserve balancing in DC microgrid systems under uncertainties like wind power and energy price variations and different types of fault events. The robust MPC algorithm considers a variable-length prediction horizon which accounts for forecasts in energy price and renewable power over one day. Furthermore, a storage system is used to increase the utility of the demands and minimize the energy costs. The algorithm is tested for multiple fault types which affect the system (line and loss of power faults).

Keywords: Energy management systems, DC microgrid, Fault events, Distributed energy resources, Robust MPC (Model Predictive Control).

1. INTRODUCTION

In view of increasing availability of renewable energy sources and political efforts to encourage clean energy, an EMS (Energy Management System) capable to adapt the grid power distribution to the renewable energy variability is required. The goal of this work is to propose a robust, optimization-based control implementation and reconfiguration for the reserve balancing in a microgrid system influenced by various types of uncertainties like wind and energy price variations or fault events.

The technical literature provides an extensive number of robust smart grids controller implementation with different goals. In Prodan and Zio [2014] a MPC algorithm for reliable microgrid energy management regarding uncertainties in the forecast is proposed and extended to fault cases in Prodan et al. [2015]. Herein the MPC algorithm considers soft constraints to enable feasibility under faults and disturbances. The algorithm enables robustness against one broken line (N-1 security). In Wu and Conejo [2017] the most critical facilities were protected to minimize worst-case loads after physical attacks (faults), such that at least N-1 security holds. Here, a tri-level min-max-min problem is used, in order to minimize possible damages (the attacker tries to maximize the damage, while the operator handles the damage minimizing the cost). In Khodabakhsh and Sirouspour [2016] the battery usage is optimized, while a multi-variant Gaussian distribution is used to model uncertainties in energy price and demands. In addition, Wytock et al. [2017] proposed a scenario-based robust MPC approach, in which the worst case of all the generated scenarios is considered. Khodaei [2014] emphasis the resiliency for smart grid under islanded conditions, while in Chen et al. [2016] the energy distribution within connected smart grids after natural disasters is analyzed. Furthermore Rahimiyan et al. [2014] provides a simple EMS and data records for the energy price and wind power for a 24 hours interval. An approximated minimax robust approach is proposed for improving the utility of demands under forecast uncertainties. Herein the approximation considers a reduced set of disturbance scenarios.

The present work extends the MPC implementation presented in Prodan et al. [2015], uses the data provided in Rahimiyan et al. [2014] and further applies robust approaches and deals with fault events. The contributions of this work are summarized in the following:

- a robust economic MPC scheme with variable prediction horizon length will be implemented to handle profile variations and maximize utility;
- branch disconnects will be treated as faults to be attenuated via fault tolerant reconfiguration strategies;
- storage charge and discharge decisions will be customized by two approaches such that a fault occurrence of finite length can be recovered from;

Hence, Section 2 details the dynamical model of the microgrid. Section 3 presents the proposed energy management system using robust optimization which is further analyzed thorough various case studies in Section 4. Finally, Section 5 draws the conclusions.

2. MICROGRID SYSTEM DESCRIPTION

We consider the dynamical model of a microgrid system which contains various loads, renewable resources and stor-

⋆ The first author would like to acknowledge the financial support of the Chair TRUST of Grenoble INP for his research stay at the Univ. Grenoble Alpes, Grenoble INP ⋆, LCIS, F-26000 Valence.
⋆ Institute of Engineering Univ. Grenoble Alpes.

Copyright lies with the authors

age units, all connected among themselves through lines (which draw power from buses) and to the utility grid. Hence, the microgrid model consists of various components (each of them characterized [1] by power, energy and adjacency matrices which link them with other grid elements):

- N_{C} consumers with: power $\boldsymbol{P}^{\mathrm{C}} \in \mathbb{R}^{N_{\mathrm{C}}}$, energy $\boldsymbol{e}^{\mathrm{C}} \in \mathbb{R}^{N_{\mathrm{C}}}$, the adjacency matrix $\boldsymbol{\Omega}_{\mathrm{B}}^{\mathrm{C}} \in \mathcal{I}^{N_{\mathrm{B}} \times N_{\mathrm{C}}}$
- N_{W} distributed energy resources with: power $\boldsymbol{P}^{\mathrm{W}} \in \mathbb{R}^{N_{\mathrm{W}}}$, energy $\boldsymbol{e}^{\mathrm{W}} \in \mathbb{R}^{N_{\mathrm{W}}}$, adjacency matrix $\boldsymbol{\Omega}_{\mathrm{B}}^{\mathrm{W}} \in \mathcal{I}^{N_{\mathrm{B}} \times N_{\mathrm{W}}}$
- N_{ST} storages with: storage energy $\boldsymbol{e}^{\mathrm{ST}} \in \mathbb{R}^{N_{\mathrm{ST}}}$, adjacency matrix $\boldsymbol{\Omega}_{\mathrm{B}}^{\mathrm{ST}} \in \mathcal{I}^{N_{\mathrm{B}} \times N_{\mathrm{ST}}}$
- N_{S} main grid connections with: power $\boldsymbol{P}^{\mathrm{S}} \in \mathbb{R}^{N_{\mathrm{S}}}$,energy $\boldsymbol{e}^{\mathrm{S}} \in \mathbb{R}^{N_{\mathrm{S}}}$, adjacency matrix $\boldsymbol{\Omega}_{\mathrm{B}}^{\mathrm{S}} \in \mathcal{I}^{N_{\mathrm{B}} \times N_{\mathrm{S}}}$
- N_{L} lines with: power $\boldsymbol{P}^{\mathrm{L}} \in \mathbb{R}^{N_{\mathrm{L}}}$, adjacency matrix $\boldsymbol{\Omega}_{\mathrm{B}}^{\mathrm{L}} \in \mathcal{I}^{N_{\mathrm{B}} \times N_{\mathrm{L}}}$
- N_{B} buses with: power $\boldsymbol{P}^{\mathrm{B}} \in \mathbb{R}^{N_{\mathrm{B}}}$

The adjacency matrices take values from $\mathcal{I} \in \{-1, 0, 1\}$, i.e., $\boldsymbol{\Omega}_B^C(i,j)$ denotes the link between the j-th consumer and the i-th battery which can be one of "consumer takes power from battery", "consumer gives power to battery" or "consumer and battery are not connected".

Hereinafter we consider discrete-time equations with the timestep τ. The storage energy $\boldsymbol{e}_\tau^{\mathrm{ST}} \in \mathbb{R}^{N_{\mathrm{ST}}}$ depends on the charge energy $\boldsymbol{e}_\tau^{\mathrm{ST},+} \in \mathbb{R}^{N_{\mathrm{ST}}}$ and discharge energy $\boldsymbol{e}_\tau^{\mathrm{ST},-} \in \mathbb{R}^{N_{\mathrm{ST}}}$ with the conversion parameters μ_1 and μ_2:

$$\boldsymbol{e}_{\tau+1}^{\mathrm{ST}} = \boldsymbol{e}_\tau^{ST} + \mu_1 \boldsymbol{e}_\tau^{\mathrm{ST},-} - \frac{\boldsymbol{e}_\tau^{\mathrm{ST},+}}{\mu_2}. \tag{1}$$

The storage capacity is bounded by the maximum storage energy $\boldsymbol{e}^{\mathrm{ST,max}}$ and a depth of discharge (DoD) of the maximum capacity:

$$DoD \cdot \boldsymbol{e}^{\mathrm{ST,max}} \leq \boldsymbol{e}_\tau^{\mathrm{ST}} \leq \boldsymbol{e}^{\mathrm{ST,max}}. \tag{2}$$

The energies corresponding to all the components of the microgrid are gathered in a vector e_τ

$$\boldsymbol{e}_\tau = [\boldsymbol{e}_\tau^{\mathrm{ST},+}, \boldsymbol{e}_\tau^{\mathrm{ST},-}, \boldsymbol{e}_\tau^{\mathrm{S}}, \boldsymbol{e}_\tau^{\mathrm{C}}, \boldsymbol{e}_\tau^{\mathrm{W}}] \tag{3}$$

$$\text{with } \boldsymbol{0} \leq \boldsymbol{e}_\tau^{\mathrm{ST},+}, \boldsymbol{e}_\tau^{\mathrm{ST},-}, \boldsymbol{e}_\tau^{\mathrm{C}}, \boldsymbol{e}_\tau^{\mathrm{W}} \tag{4}$$

and are expressed in terms of power by using the trapezoidal rule:

$$\boldsymbol{e}_\tau = \frac{\boldsymbol{P}_\tau + \boldsymbol{P}_{\tau+1}}{2}, \tag{5}$$

where the inputs and decision variables are:

$$\boldsymbol{P}_{\tau+1} = [\boldsymbol{P}_{\tau+1}^{\mathrm{ST},+}, \boldsymbol{P}_{\tau+1}^{\mathrm{ST},-}, \boldsymbol{P}_{\tau+1}^{\mathrm{S}}, \boldsymbol{P}_{\tau+1}^{\mathrm{C}}, \boldsymbol{P}_{\tau+1}^{\mathrm{W}}]. \tag{6}$$

To divide times of charge and discharge, we use an auxiliary variable $\alpha_{\tau+1} \in \{0, 1\}$ in the mixed-integer conditions:

$$0 \leq \boldsymbol{P}_{\tau+1}^{\mathrm{ST},-} \leq \alpha_{\tau+1} \boldsymbol{P}^{\mathrm{ST,max}}, \tag{7a}$$

$$0 \leq \boldsymbol{P}_{\tau+1}^{\mathrm{ST},+} \leq (1 - \alpha_{\tau+1}) \boldsymbol{P}^{\mathrm{ST,max}}. \tag{7b}$$

A sell-or-pay contract is considered for the main grid, wherein the microgrid can buy and sell energy for the current, time-variant energy price $\lambda_\tau^{\mathrm{S}}$. In this case the minimum bound $P^{\mathrm{S,min}}$ may be negative:

$$\boldsymbol{P}^{\mathrm{S,min}} \leq \boldsymbol{P}_{\tau+1}^{\mathrm{S}} \leq \boldsymbol{P}^{\mathrm{S,max}}. \tag{8}$$

[1] One or another of these variables may be ignored if not relevant for the particular grid element.

The main grid power can increase per hour by a maximum value $\Delta \boldsymbol{P}^{\mathrm{S,max}}$. In case of shutdown cycle, there exists no lower bound for the main grid power variation:

$$\boldsymbol{P}_{\tau+1}^{\mathrm{S}} - \boldsymbol{P}_\tau^{\mathrm{S}} \leq \Delta \boldsymbol{P}^{\mathrm{S,max}} \tag{9}$$

The renewable power is bounded by the available renewable power $\boldsymbol{P}^{\mathrm{AW}}$:

$$\boldsymbol{P}^{\mathrm{W,min}} \leq \boldsymbol{P}_{\tau+1}^{\mathrm{W}} \leq \boldsymbol{P}_{\tau+1}^{\mathrm{AW}} \tag{10}$$

The renewable power is bought with the constant energy price λ^{W}.

Each consumer has a power demand which lies in between known minimum (time-variant) and maximum (constant) demand bounds $\boldsymbol{P}_{\tau+1}^{\mathrm{C,min}}$, $\boldsymbol{P}^{\mathrm{C,max}}$:

$$\boldsymbol{P}_{\tau+1}^{\mathrm{C,min}} \leq \boldsymbol{P}_{\tau+1}^{\mathrm{C}} \leq \boldsymbol{P}^{\mathrm{C,max}}. \tag{11}$$

Furthermore we bound the consumption variation by:

$$\boldsymbol{r}^{\min} \leq \boldsymbol{P}_{\tau+1}^{\mathrm{C}} - \boldsymbol{P}_\tau^{\mathrm{C}} \leq \boldsymbol{r}^{\max}. \tag{12}$$

Also, the consumers have to meet a minimum daily energy consumption $\boldsymbol{e}^{\mathrm{day}}$ while, simultaneously, through an optimal scheduling, increase the grid utility. Thus, at the current time instant the sum of "already" and "to be"-consumed energies has to respect the constraint

$$\sum_{h=1}^{t-1} \boldsymbol{e}_h^{\mathrm{C}} + \sum_{h=0}^{24-t} \boldsymbol{e}_\tau^{\mathrm{C}} \geq \boldsymbol{e}^{\mathrm{day}}. \tag{13}$$

The power capacity of each line is bounded by the maximum capacity $\boldsymbol{P}^{\mathrm{L,max}}$ and minimum capacity $\boldsymbol{P}^{\mathrm{L,min}}$:

$$\boldsymbol{P}^{\mathrm{L,min}} \leq \boldsymbol{P}_{\tau+1}^{\mathrm{L}} \leq \boldsymbol{P}^{\mathrm{L,max}}. \tag{14}$$

The power balancing problem based on the so-called DC power flow equations including the line incidence matrix $\boldsymbol{\Omega}_{\mathrm{B}}^{\mathrm{L}}$ and susceptance $\boldsymbol{B}$:

$$\boldsymbol{P}^{\mathrm{L}} = \boldsymbol{B} \boldsymbol{\Omega}_{\mathrm{B}}^{\mathrm{L}\top} (\boldsymbol{\Omega}_{\mathrm{B}}^{\mathrm{L}} \boldsymbol{B} \boldsymbol{\Omega}_{\mathrm{B}}^{\mathrm{L}\top})^{-1} \boldsymbol{P}^{\mathrm{B}} \tag{15a}$$

$$\sum_b P_b^{\mathrm{B}} = 0. \tag{15b}$$

The bus injection depends on the wind, storage charge and discharge, main grid power, and the demand, where $\boldsymbol{\Omega}_{\mathrm{B}}^{(\cdot)}$ are the adjacency matrices:

$$\begin{aligned} \boldsymbol{P}^{\mathrm{B}} = {} & \boldsymbol{\Omega}_{\mathrm{B}}^{\mathrm{W}} \boldsymbol{P}^{\mathrm{W}} - \boldsymbol{\Omega}_{\mathrm{B}}^{\mathrm{C}} \boldsymbol{P}^{\mathrm{C}} \\ & + \boldsymbol{\Omega}_{\mathrm{B}}^{\mathrm{ST}} (\boldsymbol{P}^{\mathrm{ST},-} - \boldsymbol{P}^{\mathrm{ST},+}) + \boldsymbol{\Omega}_{\mathrm{B}}^{\mathrm{S}} \boldsymbol{P}^{\mathrm{S}}. \end{aligned} \tag{16}$$

Each power demand is weighted by utility $\boldsymbol{u}^\top \in \mathbb{R}^{N_{\mathrm{C}}}$, to value the worth of the consumption in comparison to the energy price.

3. ENERGY MANAGEMENT SYSTEM (EMS)

The EMS solves, at each step, a constrained optimization problem with an economic objective function, which minimizes the cost of wind λ^{W} and external grid energy, while simultaneously maximizing the utility $\boldsymbol{u}$.

$$\begin{aligned} J_t = {} & \lambda_t^{\mathrm{S}} e_t^{\mathrm{S}} - \boldsymbol{u}_t^{\mathrm{T}} \boldsymbol{e}_t^{\mathrm{C}} + \lambda^{\mathrm{W}} e_t^{\mathrm{W}} \\ & + \sum_{h=1}^{24-t} \lambda_{t+h}^{\mathrm{S}} e_{t+h}^{\mathrm{S}} - \boldsymbol{u}_{t+h}^{\mathrm{T}} \boldsymbol{e}_{t+h}^{\mathrm{C}} + \lambda^{\mathrm{W}} e_{t+h}^{\mathrm{W}}. \end{aligned} \tag{17}$$

The whole optimization problem is given by

$$\begin{aligned}
\min \quad & J_t \quad (17) && (18a)\\
\text{s.t.} \quad & \text{power balancing conditions} \quad (15),(16) && (18b)\\
& \text{storage unit dynamics} \quad (1) && (18c)\\
& \text{storage constraints} \quad (2),(7) && (18d)\\
& \text{trapezoidal rule} \quad (5) && (18e)\\
& \text{main grid constraints} \quad (8),(9) && (18f)\\
& \text{consumer constraints} \quad (11),(13),(12) && (18g)\\
& \text{power lines constraints} \quad (14) && (18h)
\end{aligned}$$

Using the utility as a time-varying weight, the value describes the worth of a particular consumption. We want to emphasize that, the objective function (17) utilizes a shrinking prediction horizon. For the current time step t, the objective function predicts $24-t$ steps into future (hence covering the remaining of the day). The constraints include the microgrid model with $\tau = t+h$, $h = 0, ..., 24-t$ and $t = 1, ..., 24$. The minimum generator power $\boldsymbol{P}^{\mathrm{W,min}}$ appears for completeness reasons but in the scheme is set to zero.

In general, the EMS is not robust under forecast disturbances. Therefore a robust control approach is required. We propose two different control approaches: the robust EMS (19) taken from Rahimiyan et al. [2014] and the minimax EMS (20). Both of them consider the same cost J_t from (17).

The robust EMS allows to set the degree of robustness by the parameters Γ^{S} and Γ^{W} (for further information see Rahimiyan et al. [2014]):

$$\begin{aligned}
\min \quad & J_t + \beta^{\mathrm{S}}\Gamma^{\mathrm{S}} + \sum_{h=1}^{24-t} \xi^{\mathrm{S}}_{t+h} && (19a)\\
\text{s.t.} \quad & \text{constraints} \quad (18) && (19b)\\
& \beta^{\mathrm{S}} + \xi^{\mathrm{S}}_{t+h} \geq (\lambda^{\mathrm{S,max}}_{t+h} - \lambda^{\mathrm{S,min}}_{t+h}) y^{\mathrm{S}}_{t+h} && (19c)\\
& -y^{\mathrm{S}}_{t+h} \leq e^{\mathrm{S}}_{t+h} \leq y^{\mathrm{S}}_{t+h} && (19d)\\
& P^{\mathrm{W}}_{t+h+1} - \frac{P^{\mathrm{AW,max}}_{t+h+1} + P^{\mathrm{AW,min}}_{t+h+1}}{2} \\
& \qquad + \beta^{\mathrm{W}}_{t+h+1}\Gamma^{\mathrm{W}}_{t+h+1} + \xi^{\mathrm{W}}_{t+h+1} \leq 0 && (19e)\\
& \beta^{\mathrm{W}}_{t+h+1} + \xi^{\mathrm{W}}_{t+h+1} \geq \frac{P^{\mathrm{AW,max}}_{t+h+1} - P^{\mathrm{AW,min}}_{t+h+1}}{2} y^{\mathrm{W}}_{t+h+1} && (19f)\\
& 1 \leq y^{\mathrm{W}}_{t+h+1} && (19g)\\
& P^{\mathrm{W}}_{t+1} \leq P^{\mathrm{AW}}_{t+1} && (19h)\\
& \beta^{\mathrm{W}}_{t+h+1}, y^{\mathrm{W}}_{t+h+1}, \xi^{\mathrm{W}}_{t+h+1}, \xi^{\mathrm{S}}_{t+h}, y^{\mathrm{S}}_{t+h}, \beta^{\mathrm{S}} \geq 0. && (19i)
\end{aligned}$$

The minimax EMS considers the worst-case scenario by using the minimax MPC algorithm [Löfberg 2003], where the available wind power and the energy price is parametrized by the minimum and maximum forecast bound under the bounded uncertainty variables w (with subscript denoting time and superscript denoting the associated variable).

$$\begin{aligned}
\min \max_{w^{\mathrm{S}}, w^{\mathrm{AW}}} \quad & J_t && (20a)\\
\text{s.t.} \quad & \text{constraints} \quad (18) && (20b)\\
& P^{\mathrm{AW}}_{t+h+1} = \frac{P^{\mathrm{AW,max}}_{t+h+1} + P^{\mathrm{AW,min}}_{t+h+1}}{2} \\
& \qquad + w^{\mathrm{AW}} \frac{P^{\mathrm{AW,max}}_{t+h+1} - P^{\mathrm{AW,min}}_{t+h+1}}{2} && (20c)\\
& -1 \leq w^{\mathrm{AW}}_{t+h+1} \leq 1 && (20d)\\
& \lambda^{\mathrm{S}}_{t+h+1} = \frac{\lambda^{\mathrm{S,max}}_{t+h+1} + \lambda^{\mathrm{S,min}}_{t+h+1}}{2} \\
& \qquad + w^{\mathrm{S}} \frac{\lambda^{\mathrm{S,max}}_{t+h+1} - \lambda^{\mathrm{S,min}}_{t+h+1}}{2} && (20e)\\
& -1 \leq w^{\mathrm{S}}_{t+h+1} \leq 1 && (20f)\\
& P^{\mathrm{W}}_{t+1} \leq P^{\mathrm{AW}}_{t+1}. && (20g)
\end{aligned}$$

Due to the good performance results of the minimax EMS, as highlighted in Section 4, the next considerations are based on the minimax EMS implementation.

Note that, when considering faults, or operating in islanded mode, the minimax EMS (20) computes no preemptive power and demand scheduling. To have reliability and feasibility, we analyze two preemptive schemes:

(1) Soft constraints for power balancing (through the slack variables $\theta_{3,(\cdot)}, \theta_{4,(\cdot)}$), where the EMS is enforced to meet the demand by the wind and storage power.

$$\begin{aligned}
\mathcal{O}^1 : \min \quad & J_t + \sum_{h=0}^{24-t} Q_3\theta_{3,t+h+1} \\
& \qquad + Q_4\theta_{4,t+h+1} && (21a)\\
\text{s.t.} \quad & \text{constraints} \quad (20) && (21b)\\
& \sum_{i=1}^{N_{\mathrm{C}}} P^{\mathrm{C},i}_{t+h+1} \leq P^{\mathrm{ST},+}_{t+h+1} + P^{\mathrm{W}}_{t+h+1} + \theta_{3,t+h+1} && (21c)\\
& P^{\mathrm{ST},-}_{t+h+1} \leq P^{\mathrm{W}}_{t+h+1} + \theta_{4,t+h+1} && (21d)\\
& 0 \leq \theta_{3,t+h+1}, \theta_{4,t+h+1}; && (21e)
\end{aligned}$$

(2) Soft constraints for demand scheduling (through the slack variable $\theta^{C}_{(\cdot)}$), where the main grid power is considered as a bounded disturbance. Soft constraints are required to be feasible regarding the worst-case scenarios.

$$\begin{aligned}
\mathcal{O}^2 : \min \max_{w^{\mathrm{PS}}} \quad & J_t + \sum_{h=0}^{24-t} Q^{\mathrm{C}}\theta^{\mathrm{C}}_{t+h+1} && (22a)\\
\text{s.t.} \quad & \text{constraints} \quad (20) && (22b)\\
& P^{\mathrm{S,unc}}_{t+h+1} = \frac{P^{\mathrm{S,max}}_{t+h+1} + P^{\mathrm{S,zero}}_{t+h+1}}{2} \\
& \qquad + w^{\mathrm{PS}} \frac{P^{\mathrm{S,max}}_{t+h+1} - P^{\mathrm{S,zero}}_{t+h+1}}{2} && (22c)\\
& P^{\mathrm{S,min}}_{t+h+1} \leq P^{\mathrm{S}}_{t+h+1} \leq P^{\mathrm{S,unc}}_{t+h+1} && (22d)\\
& -1 \leq w^{\mathrm{PS}}_{t+h+1} \leq 1 && (22e)\\
& \boldsymbol{P}^{\mathrm{C,min}}_{t+h+1} \leq \boldsymbol{P}^{\mathrm{C}}_{t+h+1} + \boldsymbol{\theta}^{\mathrm{C}}_{t+h+1} \leq \boldsymbol{P}^{\mathrm{C,max}}_{t+h+1} && (22f)\\
& 0 \leq \boldsymbol{\theta}^{\mathrm{C}}_{t+h+1} && (22g)\\
& 0 \leq \boldsymbol{P}^{\mathrm{C}}_{t+h+1} && (22h)
\end{aligned}$$

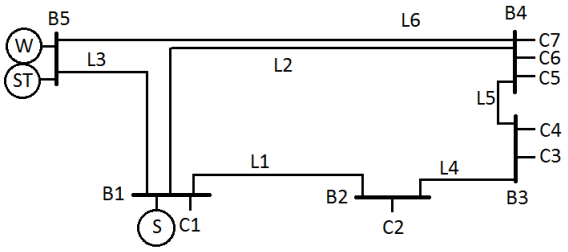

Fig. 1. 5-bus microgrid architecture.

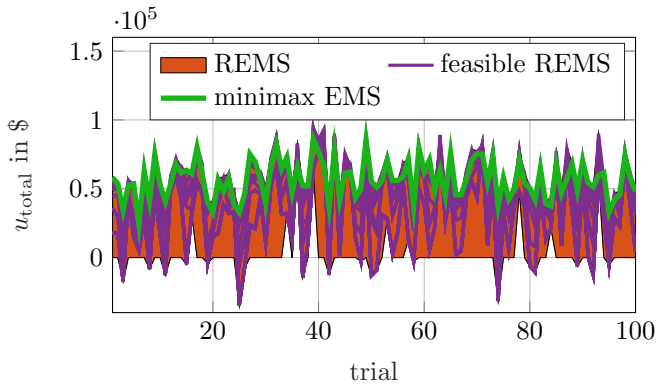

Fig. 2. Total utility of minimax MPC and robust EMS

4. CASE STUDIES

4.1 Performance over one day

For the undergoing case studies we use the 5-bus system in Fig. 1. The wind power, energy price, utility and minimum demand profiles are taken from Rahimiyan et al. [2014].

$$J = \sum_{t=1}^{24} \lambda_t^{\mathrm{S}} e_t^{\mathrm{S}} - \boldsymbol{u}_t^{\mathrm{T}} \boldsymbol{e}_t^{\mathrm{C}} + \lambda^{\mathrm{W}} e_t^{\mathrm{W}} \tag{23}$$

Regarding the forecast disturbances, we simulate the performance of the robust EMS (REMS) and the minimax EMS, where we apply randomly the minimum or maximum forecast bound for the next time step in 100 scenarios. To analyze both approaches we use the total utility (23). The results in Fig. 2 indicate that the robust EMS has a performance range which is strongly parameter-dependent (e.g., there are parameter combinations that cause infeasibility, and parameter combinations that are feasible for every scenario). Depending on the scenario, the robust EMS can lead to a better performance, than the minimax EMS. The latter is feasible in every scenario and leads to a good performance independent of the parameter choice. This is due to the good performance under disturbances that the schemes (21) and (22) have for the minimax EMS.

Considering line, storage, wind faults and the islanded mode, the overall goal is to charge preemptively the storage system, such that the necessary demand is covered. For the implementation, we use two controllers:

(1) The "healthy-mode" controller (which uses internally, for prediction, the nominal grid model). This corresponds in fact to the results presented and discussed above (Fig. 2 and the surrounding text).

Table 1. 5-bus-system: nominal Performance of preemptive schemes for grid fault

Approach	u_{total} [\$ $\cdot 10^4$]	V_0	V_1 [$\frac{\$}{\text{MWh}}$]
minimax EMS	3.92	0.035	7.66
$\mathcal{O}^1$	2.08	0.214	4.14
$\mathcal{O}^2$	3.23	0.042	6.11

(2) The "faulty-mode" controller (the grid model is changed to characterize a fault [2]). This controller becomes active whenever a fault is detected (we assume no missed faults or false alarms). Once the grid is again under nominal functioning, the EMS switches back to the healthy-mode controller.

We are interested in the advantages and shortcomings of preemptive control schemes. These strongly depend on fault type, frequency of occurrence and operational constraints (e.g., line faults do not require a charged storage system; storage and wind faults depend on the external grid power variation constraints wheneve, e.g., the EMS is bound to sell energy to the external grid).

Since each fault type is solved by specific and optimized architecture design, we hereinafter consider a limited test case: we focus on the islanded mode and consider temporary and unexpected lack of wind power as the fault.

In general, the minimax EMS does not schedule the demands and charge the storage preemptively, thus we compare two preemptive schemes in Fig. 3 under nominal conditions. The soft constrained power balancing scheme $\mathcal{O}^1$ causes a high battery usage, such that the storage charges and discharges frequently. In comparison to the minimax capacity profile $e_{\text{nom}}^{\text{ST}}$, the preemptive scheme charges earlier, while in this example the battery remains longer at the maximum capacity for the original minimax EMS. Hence the EMS schedules the demands preemptively. Scheme $\mathcal{O}^2$ charges earlier than the nominal case and remains close to being fully charged until the economic cost forces the discharge. In Tab. 1 Scheme $\mathcal{O}^1$ has a worse total utility (24) and profit (27), since the higher battery usage (26) is economically expensive.

$$u_{\text{total}} = -\sum_{t=0}^{24} [\lambda_t^{\mathrm{S}} e_t^{\mathrm{S}} + \lambda^{\mathrm{W}} e_t^{W} - \boldsymbol{u}_t^{\mathrm{T}} \boldsymbol{e}_t^{\mathrm{C}}] \tag{24}$$

$$e_{\text{total}} = \sum_{t=1}^{24} \sum_{k=1}^{N_{\mathrm{C}}} e_{k,t}^{\mathrm{C}} \tag{25}$$

$$V_0 = \frac{\sum_{t=1}^{24} e_t^{\mathrm{ST},-}}{e_{\text{total}}} \tag{26}$$

$$V_1 = \frac{u_{\text{total}}}{e_{\text{total}}} \tag{27}$$

Under unexpected islanded mode the minimax EMS predicts at hour 7 no available wind power for the next 2 hours (worst-case-scenario). Therefore a higher storage energy is required due to variation constraints on the main grid power. Scheme $\mathcal{O}^1$ is infeasible for this scenario, because

[2] For line, storage and wind faults the fault duration is unknown, so the fault is considered until the end of the day. For the islanded mode, we use a fixed fault duration of one hour.

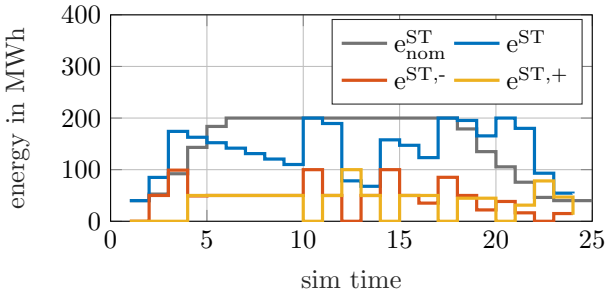

(a) Scheme $\mathcal{O}^1$.

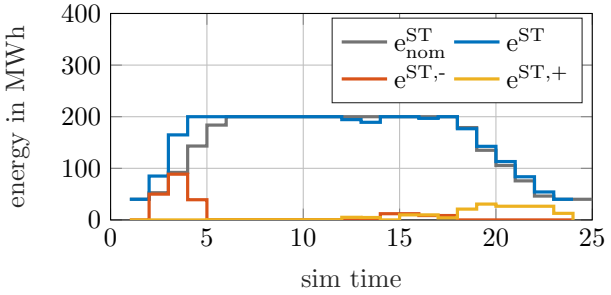

(b) Scheme $\mathcal{O}^2$.

Fig. 3. Nominal storage profile.

Table 2. 5-bus-system: performance under islanded mode.

Approach	u_{total} [\$ $\cdot 10^4$]	V_0	V_1 [$\frac{\$}{\text{MWh}}$]
Nominal	3.23	0.042	6.11
Unknown fault	2.95	0.046	5.72
Known fault	2.95	0.046	5.71

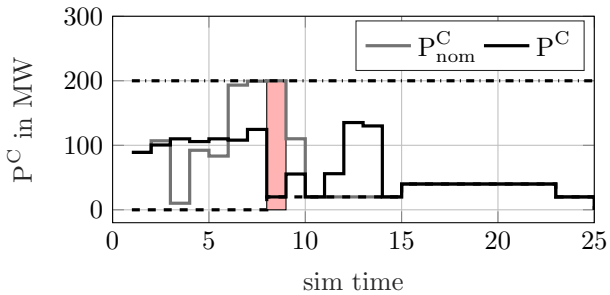

Fig. 4. Consumer 7 under fault.

EMS follows economic objectives which lead to stored energy insufficient in covering the demands. Scheme $\mathcal{O}^2$ is feasible and chooses an optimal demand schedule under fault. E.g. for consumer 7 in Fig. 4 the demand is lower before the fault appears and still receives the minimum demand under fault.

In general, we cannot a priori provide guarantees about the feasibility of Schemes $\mathcal{O}^1$ or $\mathcal{O}^2$. Scheme $\mathcal{O}^1$ has a high battery usage, which leads to a worse overall cost. Scheme $\mathcal{O}^2$ is conservative, since it considers the worst-case scenario. The economic objectives and economic soft constraints can lead to infeasible steady-states. Thus, we consider these schemes (and similar variations) as tools to be used in Monte Carlo-like analysis: multiple faults, profiles and parameters variations are considered in order

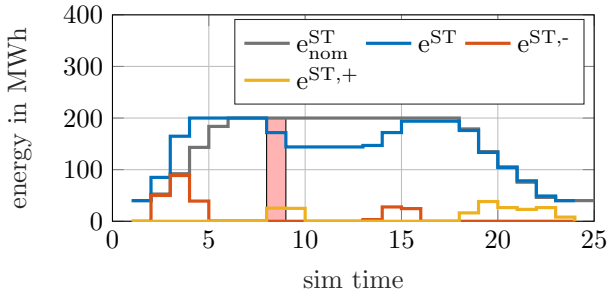

Fig. 5. Storage Energy under fault.

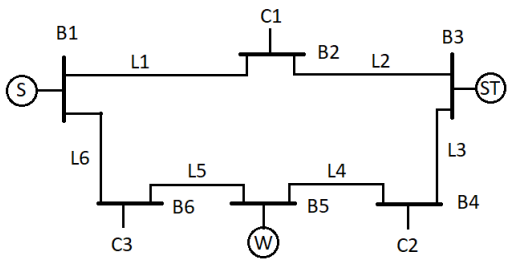

Fig. 6. 6-bus microgrid architecture.

to assess which scheme, and under which circumstances, is better-suited to a particular case.

4.2 Capacity Comparison

In the previous section, we have focused on the performance over one day with a particular model setup. For further comparisons we introduce the 6-bus-system in Fig. 6, which is a simplification of the standard IEEE 9-bus system. Arguably, the defining parameter for feasibility and reliability is the storage capacity. To analyze certain feasibility and reliability domains Fig. 7, 8 and 9 indicate the total utility as a function on fault time and storage capacity. These figures show the top-view of an 3D-plot, where the height is color-coded.

We compare the Schemes $\mathcal{O}^1$ and $\mathcal{O}^2$ with the 5-bus-system and the 6-bus-system. Infeasibility is denoted by zero. The EMS in Fig. 7 is infeasible for both systems between hour 8 for any storage capacity. There is no storage range where the EMS is feasible, for any fault time.

With scheme $\mathcal{O}^1$ we can determine a feasible area for a storage capacity between 70 and 180 MWh in Fig. 8 for the 6-bus-system. Applying the scheme $\mathcal{O}^1$ on the 5-bus-system the infeasible area increases. On the contrary, scheme $\mathcal{O}^2$ leads to a feasible range for the 5-bus-system between 0 and 50 plus 70 and 230 MWh. Although the scheme cannot provide a continuous feasible range for the 6 bus-system, it manages to minimize the infeasible areas.

5. CONCLUSION

We described a detailed microgrid model which was further employed for model-based prediction into constrained-optimization implementations of an energy management system (EMS). We have considered two variations of robust MPC and tested their feasibility and performance under nominal and fault-affected functioning. The test cases show that, even for small-scale microgrid systems

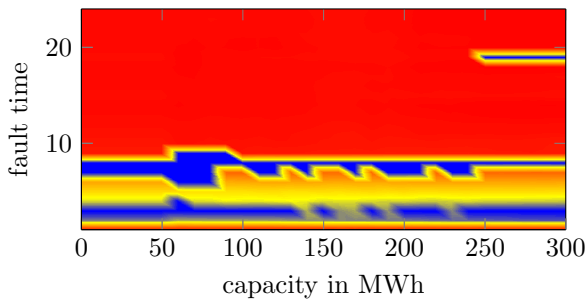

(a) 5-bus-system.

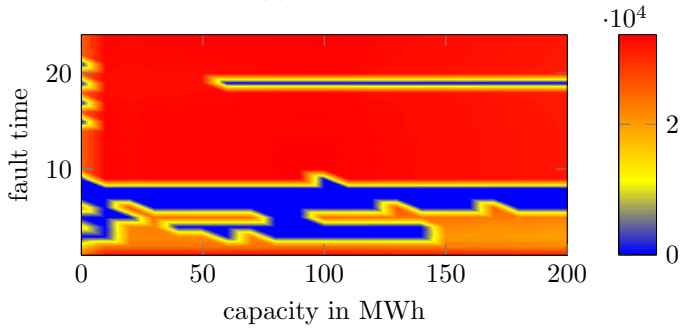

(b) 6-bus-system.

Fig. 7. Total utility depending on fault time and storage capacity with EMS. Zero indicates infeasibility.

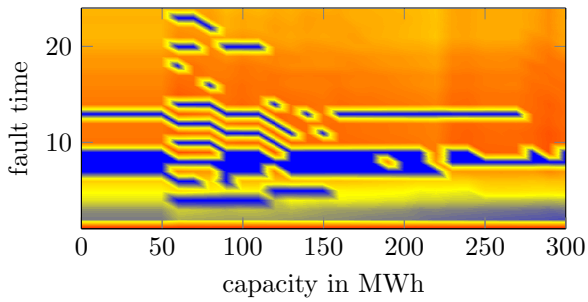

(a) 5-bus-system.

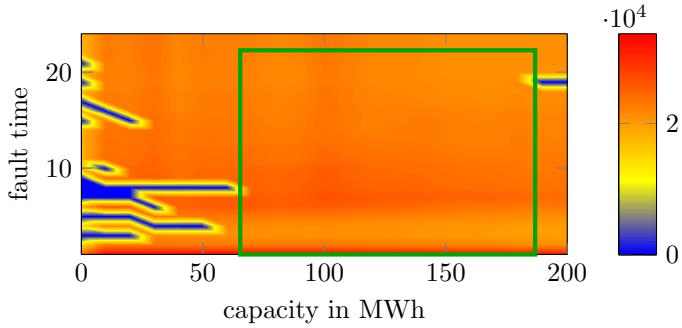

(b) 6-bus-system.

Fig. 8. Total utility depending on fault time and storage capacity with scheme $\mathcal{O}^1$; the green frame indicates storage capacities to obtain fault-time-independent feasibility. Zero indicates infeasibility.

(5 and 6-buses) the behavior is complex and is strongly influenced by the interplay between parameters, profiles and control decisions. The storage is, arguably, the most important grid component as its size and charge/discharge decisions greatly influence the performance of the EMS. Further work will focus on a priori guarantees of feasibility.

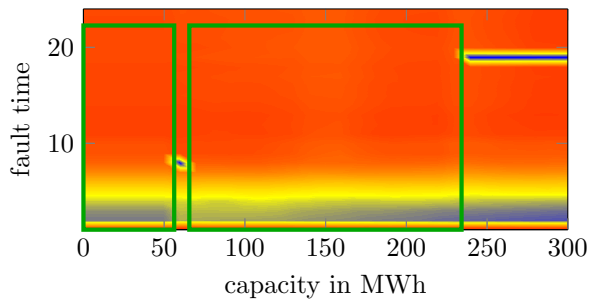

(a) 5-bus-system.

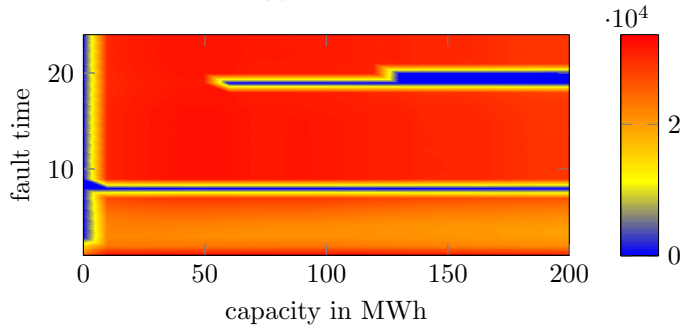

(b) 6-bus-system.

Fig. 9. Total utility depending on fault time and storage capacity with scheme $\mathcal{O}^2$; the green frame indicates storage capacities to obtain fault-time-independent feasibility. Zero indicates infeasibility.

REFERENCES

Chen, C., Wang, J., Qiu, F., and Zhao, D. (2016). Resilient distribution system by microgrids formation after natural disasters. *IEEE Transactions on Smart Grid*, 7(2), 958–966.

Khodabakhsh, R. and Sirouspour, S. (2016). Optimal control of energy storage in a microgrid by minimizing conditional value-at-risk. *IEEE Transactions on Sustainable Energy*, 7(3), 1264–1273.

Khodaei, A. (2014). Resiliency-oriented microgrid optimal scheduling. *IEEE Transactions on Smart Grid*, 5(4), 1584–1591.

Löfberg, J. (2003). *Minimax approaches to robust model predictive control*, volume 812. Linköping Univ. Electronic Press.

Prodan, I. and Zio, E. (2014). A model predictive control for reliable microgrid energy management. *Int. Journal of Electrical Power and Energy Systems*, 61(1), 399–409.

Prodan, I., Zio, E., and Stoican, F. (2015). Fault tolerant predictive control design for reliable microgrid energy management under uncertainties. *Energy*, 91, 20–34.

Rahimiyan, M., Baringo, L., and Conejo, A.J. (2014). Energy management of a cluster of interconnected price-responsive demands. *IEEE Transactions on Power Systems*, 29(2), 645–655.

Wu, X. and Conejo, A.J. (2017). An efficient tri-level optimization model for electric grid defense planning. *IEEE Transactions on Power Systems*, 32(4), 2984–2994.

Wytock, M., Moehle, N., and Boyd, S. (2017). Dynamic energy management with scenario-based robust mpc. In *IEEE American Control Conference*, 2042–2047.